Physics of Fluids

# Leidenfrost drop impact on inclined superheated substrates

Cite as: Phys. Fluids **32**, 112113 (2020); https://doi.org/10.1063/5.0027115
Submitted: 27 August 2020 • Accepted: 01 November 2020 • Published Online: 20 November 2020

Yujie Wang (王俞杰), Ayoub El Bouhali, Sijia Lyu (吕思佳), et al.

Physics of Fluids ARTICLE scitation.org/journal/phf

# Leidenfrost drop impact on inclined superheated substrates

Cite as: Phys. Fluids 32, 112113 (2020); doi: 10.1063/5.0027115
Submitted: 27 August 2020 • Accepted: 1 November 2020 •
Published Online: 20 November 2020



Yujie Wang (王俞杰),[1] Ayoub El Bouhali,[1] Sijia Lyu (吕思佳),[1,a)] Lu Yu (余璐),[2] Yue Hao (郝岳),[1] Zhigang Zuo (左志钢),[2] Shuhong Liu (刘树红),[2] and Chao Sun (孙超)[1,3]

## AFFILIATIONS

[1]Center for Combustion Energy, Key Laboratory for Thermal Science and Power Engineering of Ministry of Education, Department of Energy and Power Engineering, Tsinghua University, 100084 Beijing, China

[2]State Key Laboratory of Hydro Science and Engineering, Department of Energy and Power Engineering, Tsinghua University, 100084 Beijing, China

[3]Department of Engineering Mechanics, School of Aerospace Engineering, Tsinghua University, Beijing 100084, China

[a)]**Author to whom correspondence should be addressed:** lvsj16@mails.tsinghua.edu.cn

## ABSTRACT

In real applications, drops always impact on solid walls with various inclinations. For the oblique impact of a Leidenfrost drop, which has a vapor layer under its bottom surface to prevent its direct contact with the superheated substrate, the drop can nearly frictionlessly slide along the substrate accompanied by spreading and retracting. To individually study these processes, we experimentally observe the impact of ethanol drops on superheated inclined substrates using high-speed imaging from two different views synchronously. We first study the dynamic Leidenfrost temperature, which mainly depends on the normal Weber number $We_\perp$. Then, the substrate temperature is set to be high enough to study the Leidenfrost drop behavior. During the spreading process, drops are always kept uniform, and the maximum spreading factor $D_m/D_0$ follows a power-law dependence on the large normal Weber number $We_\perp$ as $D_m/D_0 = \sqrt{We_\perp/12+2}$ for $We_\perp \geq 30$. During the retracting process, drops with low impact velocities become non-uniform due to the gravity effect. For the sliding process, the residence time of all studied drops is nearly a constant, which is not affected by the inclination and the $We$ number. The frictionless vapor layer resulting in the dimensionless sliding distance $L/D_0$ follows a power-law dependence on the parallel Weber number $We_{||}$ as $L/D_0 \propto We_{||}^{1/2}$. Without direct contact with the substrate, the behaviors of drops can be separately determined by $We_\perp$ and $We_{||}$. When the impact velocity is too high, the drop fragments into many tiny droplets, which is called the splashing phenomenon. The critical splashing criterion is found to be $We_\perp^* \simeq 120$ or $K_\perp = We_\perp Re_\perp^{1/2} \simeq 5300$ in the current parameter regime.



## I. INTRODUCTION

Drop impact dynamics on a substrate has a wide range of industrial applications, such as spray combustion,[1] spray cooling,[2] inkjet printing,[3] spray coating,[4] and so forth. The perpendicular drop impact on solid substrates has been widely studied to reveal the complicated dynamic mechanisms between the drop and the substrate.[5–8] However, in practical applications, the drop usually impacts on the substrate obliquely. In these cases, besides spreading and rebounding, the drop slides along the inclined substrate, and the attachment of the drop to the substrate causes different impact regimes,[9–12] such as deposition, rivulet, sliding, rolling, partial rebound, and complete rebound.[10] For the droplet impacting on substrates obliquely, the properties of the substrate are very important.[12,13] Therefore, we want to know if there is no attachment between the drop and the substrate and how the drop behaves when it impacts on the inclined substrate.

A very ideal drop is the Leidenfrost drop,[14] which has a vapor layer under its bottom surface to prevent its direct contact with the heated substrate.[15,16] Thanks to the occurrence of the vapor

layer, the drop can move freely along the substrate.[17–19] Some studies have focused on a compound Leidenfrost droplet impinging on an inclined surface.[20,21] They showed the entire impacting process[20] and studied the resident time[21] of the drop. In this work, we conduct systematic experiments to deeply understand the effects of the impact velocity and the inclination of the surface on the dynamic Leidenfrost temperature and the drop impact dynamics. These results can help us adjust the range of various parameters in industrial applications. In addition, the oblique drop impact is an easy way to alter the moving direction and the shape of drops, which can be applied in spray fields.

## II. EXPERIMENTAL METHODS

The sketch of the experimental setup is shown in Fig. 1(a). An ethanol drop is generated from the tip of a blunt needle connected to a syringe pump (Harvard Apparatus PHD ULTRA) with a constant flow rate (≈0.08 ml/min). The initial diameter of the drop $D_0$ is 2.1 ± 0.1 mm. We change the height of the needle to adjust the impact velocity of the drop $U$, within the range of 0.2 m/s–3.0 m/s. The corresponding Weber number $We = \rho D_0 U^2/\sigma$ ranges from 3 to 680, where $\rho$ is the density of ethanol and $\sigma$ is the surface tension of ethanol at room temperature. Two sets of high-speed cameras (Photron FASTCAM Mini AX200 and Photron FASTCAM Mini UX100) with macro-lenses (Canon EF 24 mm–105 mm) are used to record the drop behaviors from top and side views synchronously with a frame rate of 6400 fps. Two halogen lamps are used to supply the reflected light for the top view and the backlight for the side view. Figure 1(b) shows a snapshot recorded from the top view, which displays the spreading and retracting processes of the drop. Figure 1(c) shows a snapshot recorded from the side view, which records the sliding process of the drop.

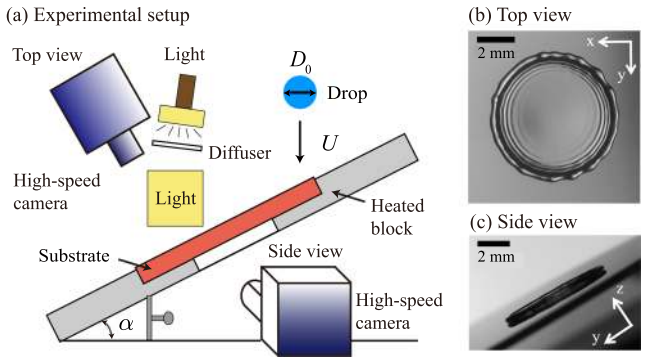


**FIG. 1**. Sketch of the experimental setup. An ethanol drop with an initial diameter $D_0 \approx 2.1$ mm impacts on a heated substrate with an inclination $\alpha$. A polished silicon wafer is used as the target substrate. In order to investigate the dynamic Leidenfrost temperature $T_L$, we use a transparent sapphire substrate to record the bottom view observation. The substrate is placed on a heated aluminum block, which is heated by four heating rods, and the temperature is controlled by a PID controller. Two sets of high-speed cameras are placed in two different directions. The corresponding images recorded from the top and the side views are shown in (b) and (c), respectively.

In our experiments, a smooth silicon wafer is used as the target substrate (the average surface roughness ≈10 nm). The diffuser scatters the light on the non-transparent substrate to facilitate clear observations from the top view. The substrate is placed on a heated aluminum block, which is heated by four heating rods. The temperature of the substrate $T_s$ is controlled by a PID controller with an accuracy of ±0.5 °C. In addition, in order to get the accurate Leidenfrost temperature, we use a transparent sapphire as another substrate. A 20 × 50 mm$^2$ rectangular hole is left at the block center, forming an observation window for the bottom view. A long-working-distance microscope with a coaxial LED lamp is placed in the bottom view. Combining side and bottom views, we can identify the boiling characteristics of drops and obtain the accurate Leidenfrost temperature $T_L$. Then, we choose a high enough substrate temperature to make sure all studied drops stay in the Leidenfrost state.

## III. RESULTS AND INTERPRETATION

We divide results and interpretation into five parts, namely, the dynamic Leidenfrost temperature, spreading dynamics, residence time, sliding distance, and splashing criterion.

### A. Dynamic Leidenfrost temperature

When a drop perpendicularly impacts on heated solid substrates, there are three different boiling regimes, i.e., contact boiling, transition boiling, and film boiling (Leidenfrost state).[8,22] These three different boiling regimes are also observed for the inclined drop impact. In order to accurately determine the Leidenfrost temperature $T_L$ (the minimum temperature of the film boiling regime), we use a transparent sapphire base as a target substrate. Combining the side and the bottom views, we can determine the accurate regime of a drop. Figure 2 shows the side-view (upper) and bottom-view (lower) recordings for a drop impact on a plate with an inclination of 30°. In the contact boiling regime [see Fig. 2(a)], the drop directly comes in contact with the substrate, as shown in the dark area from the bottom view. As the substrate temperature increases, more vapor is generated under the drop bottom; therefore, the drop only partially wets the substrates (see the dark area in the third image from the bottom view). In addition, the drop stays in an unsteady state, as shown in the side view. This regime is called transition boiling [see Fig. 2(b)]. When the substrate temperature increases beyond a critical temperature, enough vapor is generated to elevate the drop from the substrate during the whole impact process; this is called the Leidenfrost regime [see Fig. 2(c)]. The transition temperature between the transition boiling regime and the Leidenfrost regime is defined as the dynamic Leidenfrost temperature ($T_L$).

In order to obtain the dependence of the dynamic Leidenfrost temperature on impact velocity and inclination, we first fix the inclination of the substrate and that of the high-speed camera. Then, we gradually increase the surface temperature by 20 °C (the increment is 10 °C near the dynamic Leidenfrost temperature). For a fixed temperature, we vary the impact velocity by adjusting the height of the needle. The boiling process was recorded from side and bottom views. For each experimental condition (fixed

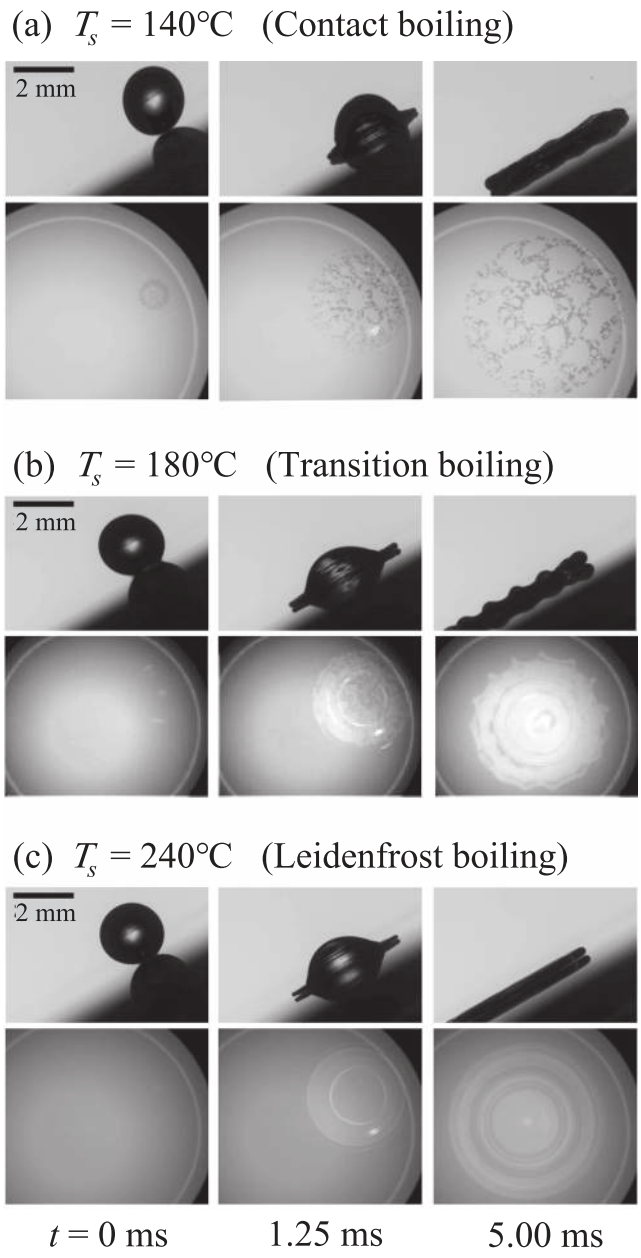


**FIG. 2**. Snapshots of ethanol drops impacting on an inclined sapphire substrate ($\alpha$ = 30°) at different substrate temperatures. Drops stay in three different boiling regimes, namely, contact boiling, transition boiling, and Leidenfrost boiling. The impact velocity $U$ is 1 m/s and Weber number $We$ is 75 for these three cases. In each group, the time sequence is 0 ms, 0.63 ms, 1.25 ms, 2.50 ms, and 5.00 ms. The images in the upper row are recorded from the side view, and lower ones are recorded from the bottom view. The dark spots in the bottom-view images indicate the liquid wetting area. The scale bars represent 2 mm.

surface temperature, inclination, and drop height), three independent experiments are conducted to eliminate the error. After completing a set of experiments of a fixed inclination, we change the inclination of the substrate and that of the high-speed camera.

In Fig. 3(a), for a fixed inclination $\alpha$, the corresponding dynamic Leidenfrost temperature $T_L$ increases with $We$ when $We$ is not too high. This dependence can be rationalized by comparing the inertial pressure of the drop and the vapor pressure. The inertial pressure of the drop is proportional to $We$, and the vapor pressure increases with $T_s$. Thus, in order to maintain a drop at high $We$ in the Leidenfrost regime, a high substrate temperature is required to produce enough vapor to overcome a large dynamic pressure of the impacting drop. As shown in Fig. 3(a), the increasing rate of $T_L$ becomes slower with increasing $We$. In addition, when $We$ is high enough, $T_L$ becomes insensitive with $We$.[22,23] The inclination angle $\alpha$ in the study is 0°, 15°, 30°, 45°, and 60°. For fixed $We$, increasing the inclination can effectively decrease $T_L$. For example, compared with drops impacting on a horizontal substrate, $T_L$ for the inclined substrate with $\alpha$ = 60° reduces roughly 100 °C when $We$ is about 100. The physical reason for the reduction in dynamic Leidenfrost temperature on the inclined substrates is due to the reduction in the

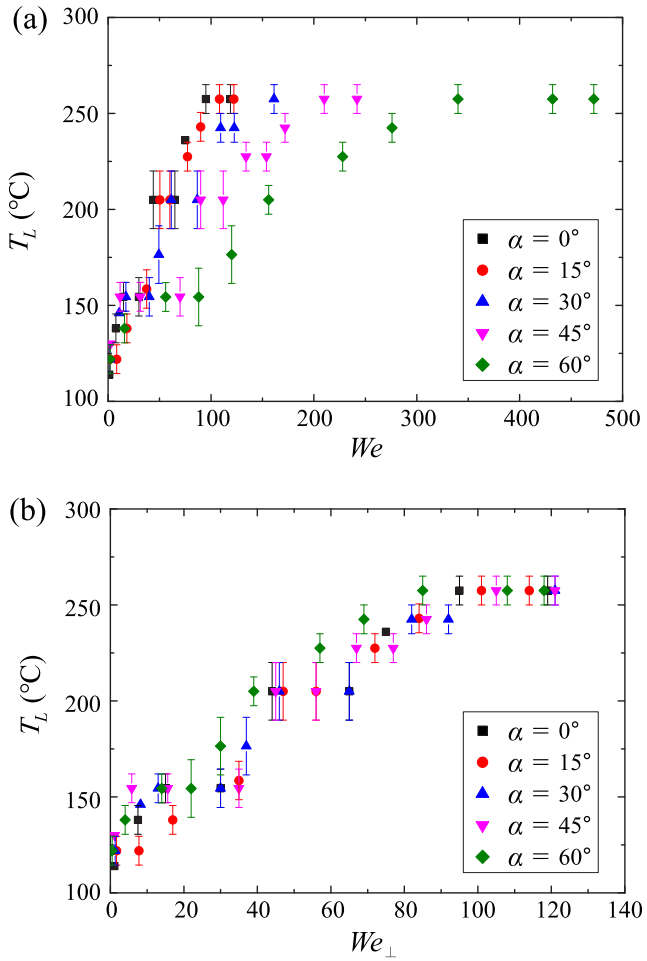


**FIG. 3**. Dynamic Leidenfrost temperature $T_L$ (the minimum temperature to maintain the drop in the Leidenfrost regime) vs (a) the Weber number $We$ and (b) the normal Weber number $We_\perp$ for different inclinations.

"effective impacting velocity," which is the normal velocity to the substrate $U_\perp = U\cos\alpha$. Using the perpendicular velocity, we define the normal Weber number as

$$We_\perp = \frac{\rho D_0 U_\perp^2}{\sigma}. \quad (1)$$

As shown in Fig. 3(b), all $T_L$ evolutions of $We_\perp$ for different inclinations collapse to a master curve, which means the dynamic Leidenfrost temperature mainly depends on the normal impact velocity. This finding indicates that it's possible to reduce the dynamic Leidenfrost temperature of an impacting drop by simply inclining the substrates due to the reduction in the normal impact velocity.

In addition, from Fig. 3(a), we know that 300 °C is higher than all Leidenfrost temperatures for our studied *We* range. Because the silicon wafer has a roughness similar to that of the sapphire wafer, we set $T_s$ = 300 °C to study Leidenfrost drops' behaviors on the silicon wafer.

### B. Leidenfrost regime: Spreading dynamics

When a drop impacts on a horizontal substrate, the spreading and retraction of the drop are nearly axisymmetric. However, when the drop impacts upon an inclined substrate at room temperature, it is found that the drop spreads asymmetrically, and it also slides along the tilting substrate.[24–27] In these cases, the impact area on the inclined surface is an approximate ellipse with a larger $D_y$ along the sliding direction and a smaller $D_x$ perpendicular to the sliding direction. The detailed model[27] was proposed to predict the time-varying asymmetric shape of the thin liquid film. At room temperature, friction plays a significant role in drop impact due to the direct contact between the drop and the substrate. However, for a Leidenfrost drop, it is not directly affected by the substrate, and therefore, the friction could be neglected.

Figure 4 shows the entire process of a Leidenfrost drop impacting on an inclined substrate. The setting parameters are $\alpha$ = 60°, $T_s$ = 300 °C, and *We* = 16. In Fig. 4(a), the side-view recording shows the definitions of the inclination $\alpha$, the sliding distance $L$, the diameter $D_y$ in the $y$ direction, and the residence time $\tau_r$. In Fig. 4(b), the top-view recording shows the definitions of the maximum spreading diameter $D_m$, the diameter $D_x$ in the $x$ direction, and the spreading and the retracting processes. It should be noticed that in the drop retraction process (from 3.75 ms to 11.25 ms), the border of the contact area can be approximated by an ellipse. The quantitative data are plotted in Fig. 5 and are discussed below. After bouncing from the substrate, the sphere drop becomes nearly cylindrical, which has a larger surface area [see red lines in the first and the last snapshots of Fig. 4(a)].

Figure 5 shows a quantitative study of $D_x/D_0$ and $D_y/D_0$ vs time for two different inclinations 45° and 60°, respectively, at three different *We* values. For all cases, drops always stay in the Leidenfrost regime. The impacting process can be recognized as two stages, i.e., the spreading process and the retracting process. As shown in Fig. 5, the temporal evolutions of the diameter in $x$ and $y$ directions during the spreading process are very close, which means the inclination of the substrate and the *We* number do not induce an azimuthal variation of the Leidenfrost drop during the spreading process. In addition, the maximum diameters are nearly the same in two directions. As expected, it increases with *We* for a fixed inclination. Comparing Fig. 5(a) with Fig. 5(b), we find the maximum spreading diameter increases with decreasing inclination at fixed

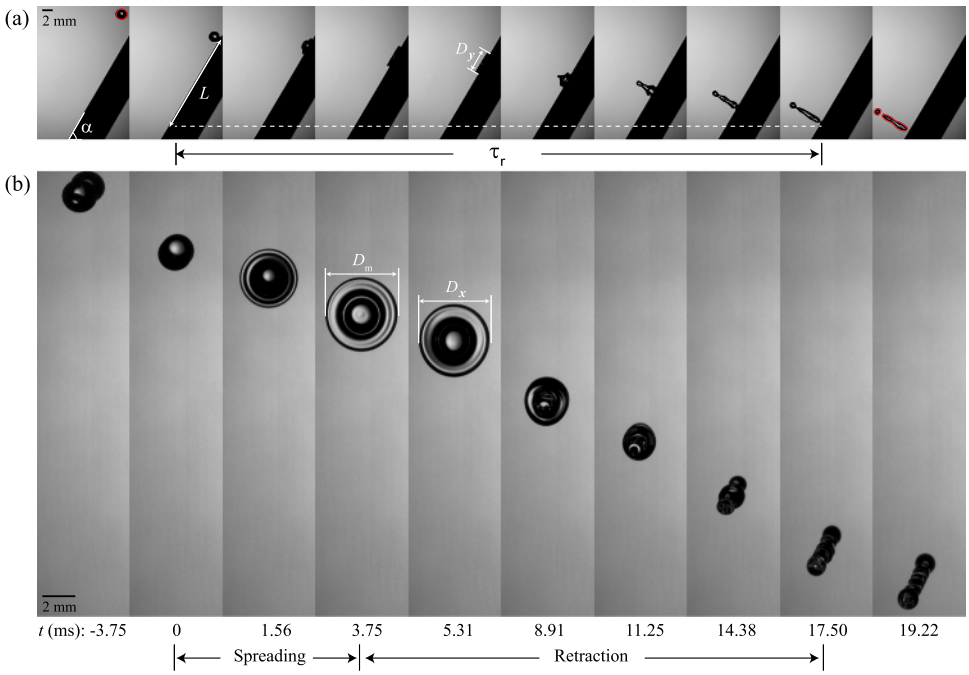


**FIG. 4**. Entire recording of a Leidenfrost drop impacting on an inclined substrate. The setting parameters are $\alpha$ = 60°, $T_s$ = 300 °C, and *We* = 16. (a) The side-view recording shows the definitions of the inclination $\alpha$, the sliding distance $L$, the diameter $D_y$ in the $y$ direction, and the residence time $\tau_r$. (b) The top-view recording shows the definitions of the maximum spreading diameter $D_m$, the diameter $D_x$ in the $x$ direction, and the spreading and the retracting processes. When the drop comes in contact with the substrate, this moment is defined as $t$ = 0. When the drop bounces off the substrate, this moment is defined as the end of the residence time. After bouncing from the substrate, the sphere drop becomes nearly cylindrical (see red lines). Scale bars represent 2 mm.

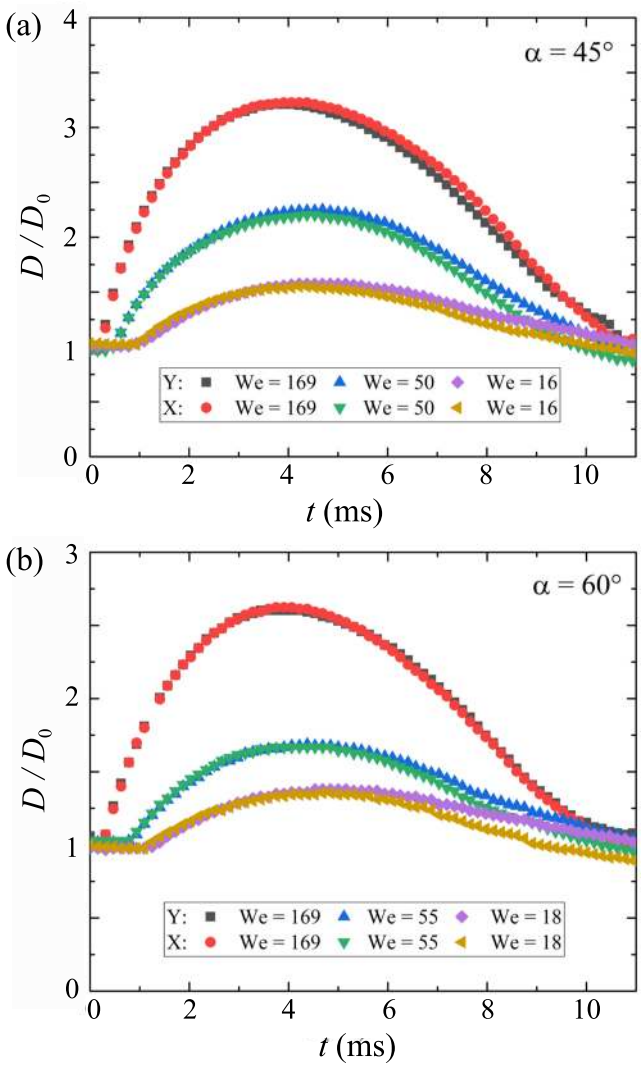


**FIG. 5**. Dimensionless spreading factor $D/D_0$ in the $x$ and $y$ directions vs time $t$ for two different inclinations. (a) $\alpha = 45°$ and (b) $\alpha = 60°$. The initial drop diameter $D_0$ is 2.1 mm.

$We = 169$. It suggests that a Leidenfrost drop can spread uniformly in two directions on inclined substrates and the maximum spreading diameter is strongly affected by the impact velocity and the substrate inclination. However, during the retraction process, it shows a slight difference in these two directions, especially for lower $We$ or a higher inclination, where the drop retracts a little more slowly in the $y$ direction. The drop retraction is primarily driven by the surface tension, which leads to a force pulling the rim of the drop inward. When the drop impacts on a flat surface, the spreading and retraction of the drop are both symmetric. However, when the drop impacts on inclined substrates, the symmetry is broken since the gravity drives the drop sliding along the slope. Some literature studies have shown that the symmetry-breaking phenomenon happens on superhydrophobic curved surfaces,[28] which could lead to the preferential fluid flows around the drop rim and then result in the asymmetric retraction of the drop. For superheated curved surfaces,[29] a similar phenomenon was also observed. In our experiments, the non-uniform rim can be detected from 3.75 ms to 11.25 ms, as shown in Fig. 4(b). To quantitatively evaluate this asymmetric phenomenon, we introduce a dimensionless number Froude number $Fr$. It is defined as $Fr = U\cos\alpha/\sqrt{gD_0}$, where $g$ is the gravitational acceleration. Decreasing $We$ or increasing the inclination can reduce $Fr$. Therefore, gravity has more time to modify the initial drop velocity during the retraction process, and gravitational effects cannot be neglected under these conditions.

We now investigate the quantitative dependence of the maximum spreading diameter $D_m$ on the $We$ number. In Fig. 6, we show a log–log plot of the maximum spreading factor $D_m/D_0$ vs $We_\perp$ for various inclinations. All spreading factors coalesce to a master curve. It implies the maximum spreading factor mainly depends on the normal Weber number $We_\perp$. $D_m/D_0$ increases with $We_\perp$, which means a larger effective normal impact velocity induces a larger spreading diameter. When we incline the substrate, the effective normal impact velocity decreases, which induces the reduction in $D_m/D_0$, suggesting less initial kinetic energy of the drop is transformed to its surface energy. Thus, we can decrease the maximum spreading diameter by increasing the inclination of the substrate. In addition, we compare our experimental results with the theoretical model for drop impact on the free-slip surface proposed by Sander *et al.*[30] The theoretical model of the dimensionless maximum spreading diameter $D_m/D_0 = \sqrt{We_\perp/12 + 2}$ for $We_\perp \geq 30$, which is shown as the black dashed line in Fig. 6. Our experimental results agree well with the theoretical model at high $We_\perp$ numbers ($We_\perp \geq 30$), which means the vapor layer can be treated as the free-slip surface. Thus, we conclude that for the Leidenfrost drop impact

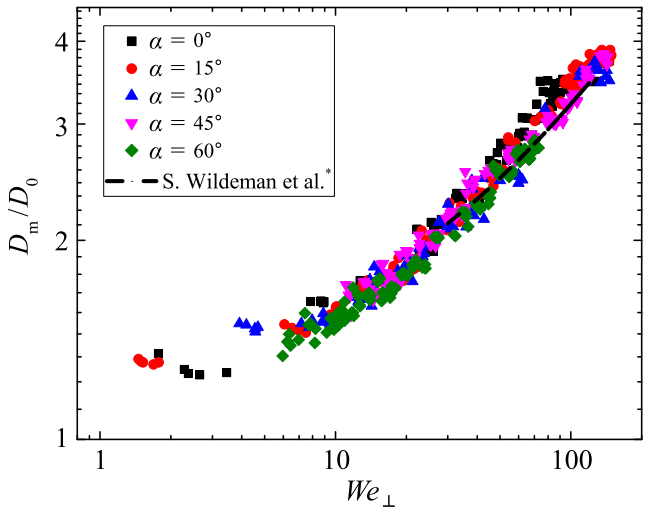


**FIG. 6**. Maximum spreading factor $D_m/D_0$ vs normal $We_\perp$ for different inclinations. $D_m/D_0$ is mainly determined by $We_\perp$. Our experimental results also fit well with the theoretical model[30] at high $We_\perp$ ($We_\perp \geq 30$), which is shown as the black dashed line.

upon an inclined substrate, the impact velocity can be decomposed to a normal component and a parallel component to the substrate, and the spreading dynamics is strongly dependent on the normal velocity.

### C. Leidenfrost regime: Residence time

When a Leidenfrost drop impacts upon a superheated substrate, it first deforms and radially spreads on the substrate. We define the moment the drop comes in contact with the substrate as the start moment of the contact time. When the impact velocity is not too high, the integral drop bounces off the substrate. Otherwise, it fragments into a lot of tiny drops (splashing). Here, we focus on the regime where the drop spreads and bounces off the substrate without the splashing. The moment that drop bounces off the substrate is the end moment of the contact time. The period between the start and the end of the contact time is the residence time $\tau_r$. For drop impact on substrates at room temperature, the attachment between the drop and the substrate causes the drop to become non-axisymmetric and then reduces the residence time of the drop.[12] Hence, we want to know if there is no attachment between the drop and the substrate and what parameters determine the residence time of a Leidenfrost drop. Normally, the residence time of a drop impact on an unheated superhydrophobic substrate or a horizontal superheated substrate is connected to that of a freely oscillating drop.[31,32] In the limit of low viscosity, the residence time can be obtained by balancing the inertia force with the capillary force. With the prefactor calculated by Rayleigh,[33] the residence time of a freely oscillating drop is given as

$$\tau_r = \frac{\pi}{4}\sqrt{\frac{\rho D_0^3}{\sigma}}. \tag{2}$$

In our experiments, the drop size $D_0$ is a constant about 2.1 mm (±0.1 mm), and the corresponding $\tau_r \simeq 15.85$ ms. $\rho_b$ and $\sigma_b$ are the density and the surface tension of ethanol at the boiling point, respectively. When the impact velocity is limited to the regime without the splashing formation, the residence time $\tau_r$ vs $We$ for a Leidenfrost drop is as shown in Fig. 7. For different impact velocities and inclinations, the residence time of a Leidenfrost drop is nearly constant, 17 ms, and $\tau_r/\tau_0 \simeq 1.07$, which is also observed by Tran *et al.*[32] The inset shows $\tau_r$ does not depend on $We_\perp$. It suggests that the capillary oscillation determines the residence time of a Leidenfrost drop impact on inclined substrates.

### D. Leidenfrost regime: Sliding distance

In previous sections, we draw the conclusion that the spreading dynamics is strongly determined by the normal velocity of the Leidenfrost drop. In this section, we focus on the effect of the parallel velocity of an impacting Leidenfrost drop. As shown in Fig. 4, besides the spreading and retracting processes, the drop slides along the substrate due to the parallel velocity. In addition, the existence of the vapor layer prevents the drop from directly coming in contact with the substrate. Then, the shear stresses acting on the drop bottom can be neglected.

To quantitatively analyze the sliding behaviors, we define the sliding distance $L$ as the length that a drop moves along the substrate during the residence time. In Fig. 8, we show a log–log plot of the dimensionless slide distance $L/D_0$ as a function of the parallel Weber number for different inclined substrates. The parallel Weber number $We_{||}$ is defined as

$$We_{||} = \frac{\rho D_0 U_{||}^2}{\sigma}, \tag{3}$$

where the parallel velocity $U_{||} = U \sin\alpha$.

All data collapse to a master curve for different inclinations. The scaling of the dimensionless sliding distance $L/D_0$ is close to the 1/2-scaling of $We_{||}$. On the basis of the free-slip boundary condition,

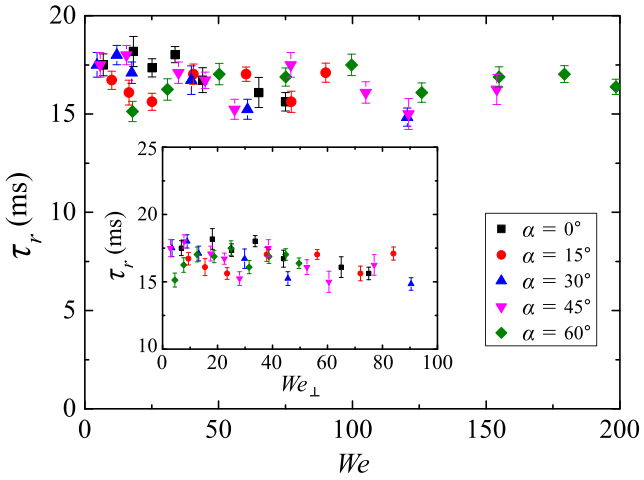


**FIG. 7.** Residence time $\tau_r$ of a Leidenfrost drop on substrates with various inclinations vs $We$. The inset plots $\tau_r$ vs $We_\perp$.

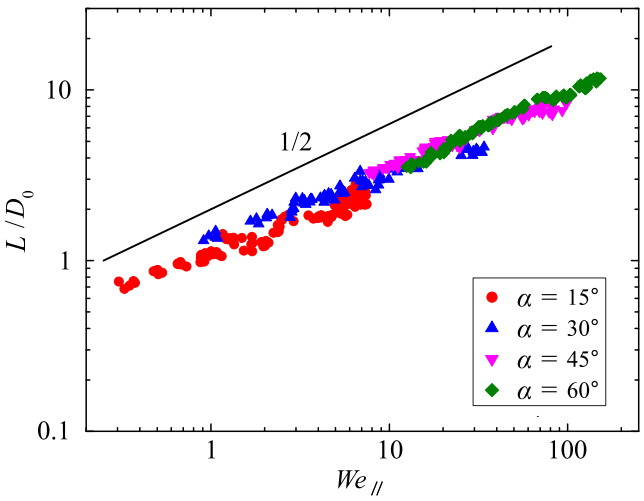


**FIG. 8.** Dimensionless sliding distance $L/D_0$ vs parallel Weber number $We_{||}$ for different inclinations. The solid line represents the scaling law in Eq. (6), $L/D_0 \propto We_{||}^{1/2}$, resulting from the free-slip boundary condition.

we can assume that the drop slides on the inclined surface with the initial velocity $v_0 = U \sin\alpha$ and with the acceleration $a = g \sin\alpha$. The sliding distance could be expressed as

$$L = v_0\tau_r + \frac{1}{2}a\tau_r^2 = \tau_r U \sin\alpha + \frac{\tau_r^2}{2} g \sin\alpha. \quad (4)$$

In our experiments, $\tau_r \simeq 15.85$ ms, and the range of velocity is 0.2 m/s–3.0 m/s. Comparing the two terms in Eq. (4), the ratio can be calculated by

$$\frac{v_0\tau_r}{\frac{1}{2}a\tau_r^2} = \frac{2U}{\tau_r g}, \quad (5)$$

which ranges from 2.56 to 33.33. It means the initial parallel velocity dominates the sliding distance in the current parameters.

For high impact velocities, we can neglect the gravitational acceleration. Then, the dimensionless sliding distance is

$$L/D_0 \approx \frac{v_0\tau_r}{D_0} \propto We_{\parallel}^{1/2}. \quad (6)$$

Thus, we conclude that the parallel velocity component contributes to the sliding process of a Leidenfrost drop on the substrate. The drop dynamics can be analyzed by decomposing the impact velocity into normal velocity and parallel velocity, which independently influence the spreading process and sliding process, respectively.

### E. Splashing criterion

When the impact velocity of a drop increases further, the surface tension cannot keep the drop integral anymore. As shown in the right-sided image of Fig. 9(a), the drop may fragment into tiny drops, violently ejecting radially outward, which is called the splashing phenomenon. When the drop can still keep the integral and no tiny drops occur, we call it the deposition state [see the left-sided image of Fig. 9(a)].

A drop impact on inclined substrates at room temperature is asymmetrical, and the parallel velocity component also affects the splashing threshold.[34] However, in our experiments, due to the high normal impact velocity in the splashing state, the Leidenfrost drop is always kept symmetrical before splashing. In addition, the drop splashing criterion is mainly controlled by the normal velocity component;[35] a phase diagram of the drop state vs $We_\perp$ is plotted to find the critical splashing criterion. As shown in Fig. 9(b), the drop stays in the deposition state for small $We_\perp$. When $We_\perp$ increases above a critical value, the drop enters the splashing state, and critical $We_\perp^* \simeq 120$ is nearly independent of the substrate inclinations, which agrees well with the model proposed by Riboux and Gordillo[36] To date, it has been found that the splashing threshold is also dependent on experimental conditions such as the surrounding pressure,[35,37,38] liquid properties,[39] substrate roughness,[37,40] and substrate temperature.[36]

Another quantity on the splashing threshold is the splashing parameter $K_\perp = We_\perp Re_\perp^{1/2}$.[41] Here, $Re_\perp$ is the normal Reynolds number of the drop. $Re_\perp$ is defined as $\rho U_\perp D_0/\mu$, where $\mu$ is the dynamic viscosity of the liquid. In Fig. 9(c), we find this normal splashing parameter $K_\perp \simeq 5300$ is nearly a constant for different inclinations

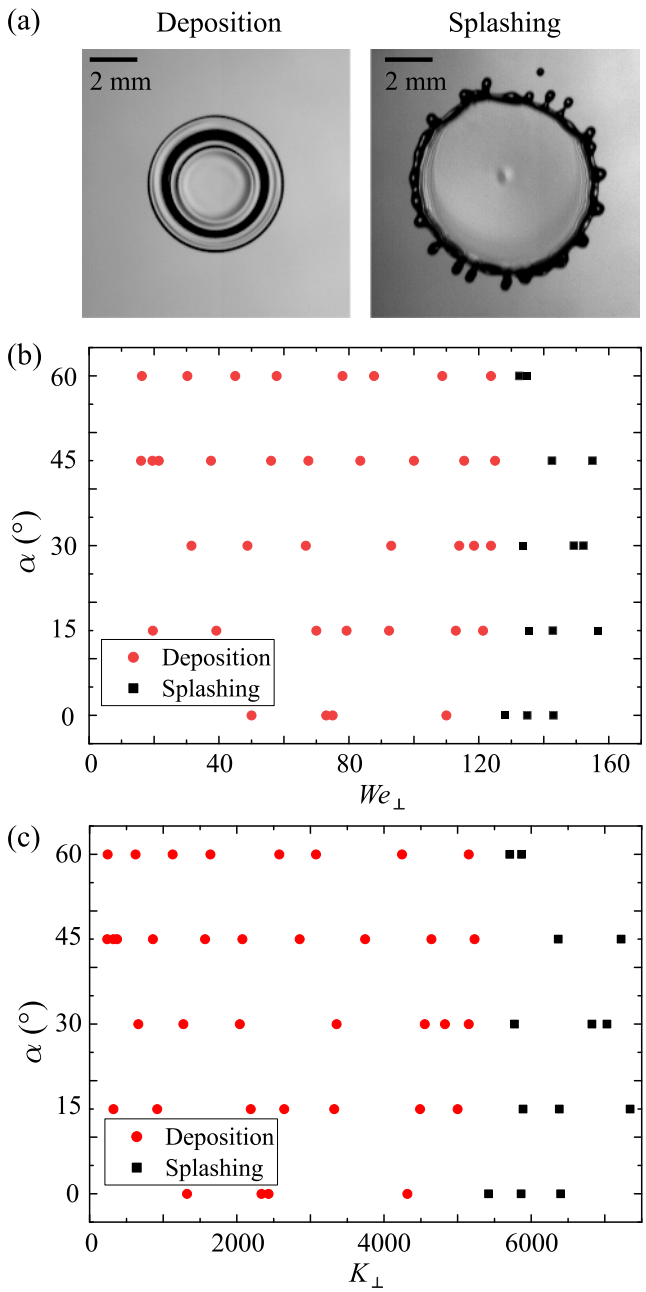


**FIG. 9.** Critical splashing criterion. (a) Top-view observes the deposition and the splashing states. Scale bars represent 2 mm. (b) A phase diagram of the drop state vs $We_\perp$ for various inclinations is plotted to find the critical splashing criterion. The critical splashing criterion $We_\perp^* \simeq 120$. (c) The critical splashing criterion is $K_\perp = We_\perp Re_\perp^{1/2} \simeq 5300$.

in the current parameter regime. The existence of the vapor layer prevents the Leidenfrost drop from directly coming in contact with the substrate. Therefore, the velocity field of the lamella is apparently different from drop impact on the surface at room temperature. This

difference results in the different splashing threshold compared with the previous results.[34,35]

## IV. DISCUSSION AND CONCLUSIONS

In this paper, we investigate the impact of ethanol drops on horizontal and inclined superheated substrates. On the horizontal and inclined substrates, there are three different boiling regimes, which are contact boiling, transition boiling, and Leidenfrost boiling. We use the bottom view to determine the wetting area and therefore obtain the dynamic Leidenfrost temperature $T_L$ for various inclinations. The results show that $T_L$ increases with $We$ for a fixed inclination $\alpha$. When fixing $We$, $T_L$ decreases with $\alpha$. When plotting the relation between $T_L$ and $We_\perp$, it is clear that $T_L$ is mainly determined by $We_\perp$.

We also investigate the spreading and retracting dynamics of Leidenfrost drops. During the spreading process, drops spread uniformly even for different inclinations. However, in the retraction process, due to the symmetry-breaking surfaces, drops tend to retract nonuniformly (slowly in the sliding direction), especially for the lower impact velocity and the higher inclined angle. We introduce a dimensionless number $Fr$ to evaluate the effect of the gravity. When $Fr$ is smaller, the gravity has more influence on modification of the drop initial velocity, and therefore, the gravity could not be neglected. The dimensionless maximum spreading factor $D_m/D_0$ is mainly determined by the normal Weber number $We_\perp$, and it fits well with the relation $D_m/D_0 = \sqrt{We_\perp/12 + 2}$ $(We_\perp > 30)$ proposed by Sander *et al.*,[30] which assumes the boundary condition of the drop is free-sliding. This model was built based on the energy budget and dissipation mechanisms, and it breaks down for $We_\perp > 30$ since the initial kinetic energy is mainly transformed into surface energy and the flow is too complex to characterize in general. The residence time $\tau_r$ of the drop is approximately related to the capillary time of a drop, which is nearly a constant and independent of impact velocity and inclination. Besides the spreading and retracting process, the drop also slides along the substrate. For high impact velocities, we can neglect the gravitational acceleration. Then, the dimensionless sliding distance is $L/D_0 \sim We_{||}^{1/2}$. When we further increase the impact velocity, the drop fragments into many tiny droplets, which is called the splashing phenomenon. The critical splashing criterion is found to be $We_\perp^* \simeq 120$ or $K_\perp \simeq 5300$. Critical $We_\perp$ for splashing agrees well with the model proposed by Riboux and Gordillo.[36]

Thanks to the existence of the vapor film, the dynamics of a Leidenfrost drop impacting on inclined surfaces could be decomposed into two components, the normal component and the parallel component, which could be described by the normal Weber number $We_\perp$ and the parallel Weber number $We_{||}$, respectively. Except drops having very large $\alpha$ or very low $We$, these two processes in orthogonal directions are nearly independent. Then, we can change the spreading diameter and the sliding distance by easily changing the inclination, which can help us adapt to the range of various parameters in industrial applications. In addition, an inclined superheated substrate is a very convenient tool to change the shape and the moving direction of a drop. After bouncing from the substrate, the sphere drop becomes nearly cylindrical, which has a larger surface area. It can be used in many applications, such as improving the combustion efficiency of fuel sprays, improving the reaction efficiency of chemical reagents, changing the mark of the spray coating, and so forth.

## ACKNOWLEDGMENTS

We gratefully acknowledge D. Lohse, H. A. Stone, and H. Xu for fruitful discussions. This work was supported by the Natural Science Foundation of China, under Grant Nos. 11861131005 and 11988102.

## DATA AVAILABILITY

The data that support the findings of this study are available from the corresponding author upon reasonable request.

## REFERENCES

[1] A. L. N. Moreira, A. S. Moita, and M. R. Panão, "Advances and challenges in explaining fuel spray impingement: How much of single droplet impact research is useful?," Prog. Energy Combust. Sci. **36**, 554–580 (2010).
[2] J. Kim, "Spray cooling heat transfer: The state of the art," Int. J. Heat Fluid Flow **28**, 753–767 (2007).
[3] B. Derby, "Inkjet printing of functional and structural materials: Fluid property requirements, feature stability, and resolution," Annu. Rev. Mater. Res. **40**, 395–414 (2010).
[4] R. Andrade, O. Skurtys, and F. Osorio, "Drop impact behavior on food using spray coating: Fundamentals and applications," Food Res. Int. **54**, 397–405 (2013).
[5] C. Josserand and S. T. Thoroddsen, "Drop impact on a solid surface," Annu. Rev. Fluid Mech. **48**, 365–391 (2016).
[6] R. Rioboo, C. Tropea, and M. Marengo, "Outcomes from a drop impact on solid surfaces," Atomization Sprays **11**(2), 155 (2001).
[7] P. R. Gunjal, V. V. Ranade, and R. V. Chaudhari, "Dynamics of drop impact on solid surface: Experiments and VOF simulations," AIChE J. **51**, 59–78 (2005).
[8] T. Tran, H. J. J. Staat, A. Prosperetti, C. Sun, and D. Lohse, "Drop impact on superheated surfaces," Phys. Rev. Lett. **108**, 036101 (2012).
[9] Y. H. Yeong, J. Burton, E. Loth, and I. S. Bayer, "Drop impact and rebound dynamics on an inclined superhydrophobic surface," Langmuir **30**, 12027–12038 (2014).
[10] C. Antonini, F. Villa, and M. Marengo, "Oblique impacts of water drops onto hydrophobic and superhydrophobic surfaces: Outcomes, timing, and rebound maps," Exp. Fluids **55**, 1713 (2014).
[11] Š. Šikalo, C. Tropea, and E. Ganić, "Impact of droplets onto inclined surfaces," J. Colloid Interface Sci. **286**, 661–669 (2005).
[12] R. Zhang, P. Hao, and F. He, "Drop impact on oblique superhydrophobic surfaces with two-tier roughness," Langmuir **33**, 3556–3567 (2017).
[13] N. Sahoo, G. Khurana, A. R. Harikrishnan, D. Samanta, and P. Dhar, "Post impact droplet hydrodynamics on inclined planes of variant wettabilities," Eur. J. Mech., B: Fluids **79**, 27–37 (2020).
[14] B. S. Gottfried, C. J. Lee, and K. J. Bell, "The Leidenfrost phenomenon: Film boiling of liquid droplets on a flat plate," Int. J. Heat Mass Transfer **9**, 1167–1188 (1966).
[15] J. G. Leidenfrost, *De Aquae Communis Nonnullis Qualitatibus Tractatus* (Ovenius, Duisburg, 1756).
[16] D. Quéré, "Leidenfrost dynamics," Annu. Rev. Fluid Mech. **45**, 197–215 (2013).
[17] I. U. Vakarelski, J. O. Marston, D. Y. Chan, and S. T. Thoroddsen, "Drag reduction by Leidenfrost vapor layers," Phys. Rev. Lett. **106**, 214501 (2011).
[18] D. Saranadhi, D. Chen, J. A. Kleingartner, S. Srinivasan, R. E. Cohen, and G. H. McKinley, "Sustained drag reduction in a turbulent flow using a low-temperature Leidenfrost surface," Sci. Adv. **2**, e1600686 (2016).
[19] Z. Yu, Y. Ge, and L.-S. Fan, "Multi-scale simulation of oblique collisions of a droplet on a surface in the Leidenfrost regime," Chem. Eng. Sci. **62**, 3462–3472 (2007).

[20]S.-L. Chiu and T.-H. Lin, "Experiment on the dynamics of a compound drop impinging on a hot surface," Phys. Fluids **17**, 122103 (2005).
[21]R.-H. Chen, S.-L. Chiu, and T.-H. Lin, "Resident time of a compound drop impinging on a hot surface," Appl. Therm. Eng. **27**, 2079–2085 (2007).
[22]M. Shirota, M. A. J. van Limbeek, C. Sun, A. Prosperetti, and D. Lohse, "Dynamic Leidenfrost effect: Relevant time and length scales," Phys. Rev. Lett. **116**, 064501 (2016).
[23]M. Khavari, C. Sun, D. Lohse, and T. Tran, "Fingering patterns during droplet impact on heated surfaces," Soft Matter **11**, 3298–3303 (2015).
[24]S. Leclear, J. Leclear, Abhijeet, K. C. Park, and W. Choi, "Drop impact on inclined superhydrophobic surfaces," J. Colloid Interface Sci. **461**, 114–121 (2016).
[25]C. Shen, C. Yu, and Y. Chen, "Spreading dynamics of droplet on an inclined surface," Theor. Comput. Fluid Dyn. **30**, 237–252 (2016).
[26]H. Wang, C. Liu, H. Zhan, and Y. Liu, "Droplet asymmetric bouncing on inclined superhydrophobic surfaces," ACS Omega **4**, 12238–12243 (2019).
[27]P. García-Geijo, G. Riboux, and J. M. Gordillo, "Inclined impact of drops," J. Fluid Mech. **897**, A12 (2020).
[28]Y. Liu, M. Andrew, J. Li, J. M. Yeomans, and Z. Wang, "Symmetry breaking in drop bouncing on curved surfaces," Nat. Commun. **6**, 10034 (2015).
[29]C. Guo, Y. Sun, and D. Zhao, "Experimental study of droplet impact on superheated cylindrical surfaces," Exp. Therm. Fluid Sci. **121**, 110263 (2021).
[30]W. Sander, V. C. Willem, S. Chao, and L. Detlef, "On the spreading of impacting drops," J. Fluid Mech. **805**, 636–655 (2016).
[31]D. Richard, C. Clanet, and D. Quéré, "Contact time of a bouncing drop," Nature **417**, 811 (2002).
[32]T. Tran, H. J. J. Staat, A. Susarrey-Arce, T. C. Foertsch, A. van Houselt, H. J. G. E. Gardeniers, A. Prosperetti, D. Lohse, and C. Sun, "Droplet impact on superheated micro-structured surfaces," Soft Matter **9**, 3272–3282 (2013).
[33]Lord Rayleigh, "On the capillary phenomena of jets," Proc. R. Soc. London **29**, 71–97 (1879).
[34]J. C. Bird, S. S. H. Tsai, and H. A. Stone, "Inclined to splash: Triggering and inhibiting a splash with tangential velocity," New J. Phys. **11**, 063017 (2009).
[35]J. Hao, J. Lu, L. Lee, Z. Wu, G. Hu, and J. Floryan, "Droplet splashing on an inclined surface," Phys. Rev. Lett. **122**, 054501 (2019).
[36]G. Riboux and J. M. Gordillo, "Maximum drop radius and critical Weber number for splashing in the dynamical Leidenfrost regime," J. Fluid Mech. **803**, 516–527 (2016).
[37]P. Tsai, R. C. A. van der Veen, M. van de Raa, and D. Lohse, "How micropatterns and air pressure affect splashing on surfaces," Langmuir **26**, 16090–16095 (2010).
[38]L. Xu, W. W. Zhang, and S. R. Nagel, "Drop splashing on a dry smooth surface," Phys. Rev. Lett. **94**, 184505 (2005).
[39]D. G. K. Aboud, M. J. Wood, and A.-M. Kietzig, "Influence of liquid properties on the oblique splashing threshold of drops," Phys. Fluids **32**, 061402 (2020).
[40]H. Kim, U. Park, C. Lee, H. Kim, M. Hwan Kim, and J. Kim, "Drop splashing on a rough surface: How surface morphology affects splashing threshold," Appl. Phys. Lett. **104**, 161608 (2014).
[41]S. T. Thoroddsen, M.-J. Thoraval, K. Takehara, and T. Etoh, "Droplet splashing by a slingshot mechanism," Phys. Rev. Lett. **106**, 034501 (2011).